Journal of Environmental Chemical Engineering 10 (2022) 107926

Contents lists available at ScienceDirect

Journal of Environmental Chemical Engineering

journal homepage: www.elsevier.com/locate/jece

Effect of amino acids on the stability of anionic pollutants in fly ash blended cement

Mengmeng Wang , Keiko Sasaki *

Department of Earth Resources Engineering, Kyushu University, Fukuoka 819-0395, Japan

ARTICLE INFO

Editor: Fumitake Takahash

Keywords:
Fly ash
Cement
Anionic pollutants
Dissolution test
Amino acids

ABSTRACT

Fly ash has been used as a cementitious material for solid wastes immobilization. However, fly ash typically contains the hazardous elements Se, Cr, As, and B, and the leachability of these anions is a concern for its reuse. In this study, five amino acids were selected as models of simplified natural organic matter (NOM) in the pedosphere to modify the dissolution tests of Se, Cr, As, and B in ground fly ash blended cement. At the initial pH of 4.7, hydrocalumite and ettringite were easily dissolved, so Ca salt precipitates played an important role in immobilizing oxyanions. However, the stability of Ca salts was weakened by the ligand-promoted dissolution mechanism. In particular, the formation of complexes of H_2Asp and HGly with Ca^{2+} promoted the release of Se, Cr, and As. H_2Cys, on the other hand, acted as a reducing reagent to suppress Se and Cr mobility. At the initial pH of 12.0, the stable formation of hydrocalumite and ettringite effectively immobilized the anionic species. Under this condition, aside from the complexation of amino acids with Ca^{2+}, the ion exchange between deprotonated amino acids and oxyanions in hydrocalumite interlayer may also threaten the stability of undesirable anionic species. However, the adsorption of amino acids on the surface of ettringite and hydrocalumite may inhibit their dissolution, resulting in a decrease in Se, Cr, As, and B release. This work provides a reference for understanding the stability of undesirable anionic pollutants in fly ash blended cement when they are exposed to geochemical environments.

1. Introduction

Coal fly ash is one of the residues of coal combustion that accounts for approximately 70% of coal ash waste [1–4]. The rich amount of calcium oxide (CaO), silica (SiO_2), alumina (Al_2O_3), and iron oxide (Fe_2O_3) in fly ash make it possible to be used as a supplementary cementitious material by reacting fly ash with water or an activator to produce Portland cement concrete [5–7]. The compressive strength of Portland cement concrete can be greatly enhanced after adding fly ash, especially the component of CaO in fly ash [8,9]. Moreover, the release of pollutants from solid wastes can be inhibited by the hydration products that are generated when fly ash reacts with water [10,11]. These hydration products can be used in waste solidification/stabilization (S/S) to reuse waste resources [12,13]. However, the usage of fly ash in cement may cause environmental contamination problems because they usually contain hazardous elements such as B, F, V, Cr, Ni, Cu, As, Se, Mo, Cd, Pb, and Hg [14–18]. Among these elements, Se, Cr, As, and B have attracted substantial attention due to the high mobility and chemical toxicity of their anionic species [17,19].

Hydrocalumite ($Ca_4Al_2(OH)_{12}SO_4{\cdot}6\ H_2O$,AFm) and ettringite ($Ca_6Al_2(OH)_{12}(SO_4)_3{\cdot}26\ H_2O$, AFt) are the main products of cement hydration, and strongly contribute to the S/S process of anionic species [17,19]. The addition of Ca is related to the formation of ettringite, hydrocalumite, and Ca salts. In addition, the concentration of Ca affects the alkalinization condition of the hydration system, where the vast majority of hazardous elements exhibit pH-dependent solubility [13, 20–22]. As a result, studies on various Ca additives have been conducted to explore their roles in immobilization. Reardon and Valle [20] used calcined dolomite to reduce the dissolved concentrations of oxyanions from fly ash, and the results revealed that the formation of hydrocalumite and hydrotalcite was the main suppression mechanism. Guo et al. [19] focused on the mixing of different Ca sources, including, lime, gypsum, slag, and 60% hydroxylated calcined dolomite, with coal fly ash. The results showed that the addition of Ca not only served as the alkaline source but also contributed to the precipitation of Ca salts, such as $CaCrO_4$, $CaSeO_3$, and $Ca_3(AsO_4)_2$. However, the mobility of anions can be affected by changes in pH and NOM when cementitious materials are exposed to geochemical environments. pH is one of the most

* Corresponding author.
E-mail addresses: wang@mine.kyushu-u.ac.jp (M. Wang), keikos@mine.kyushu-u.ac.jp (K. Sasaki).

https://doi.org/10.1016/j.jece.2022.107926
Received 15 February 2022; Received in revised form 20 April 2022; Accepted 14 May 2022
Available online 16 May 2022

Table 1
Elemental compositions of fly ash in the present work (wt%).

MgO	Al_2O_3	SiO_2	P_2O_5	SO_3	K_2O	CaO	TiO_2	MnO	Fe_2O_3
0.70	24.68	59.44	0.53	0.73	1.87	2.30	2.23	0.08	6.69

Table 2
Leaching results of undesirable elements from the original fly ash (ppm).

	Cr	As	Se	B
Fly ash	0.240	0.025	0.57	2.1
MCLs*	≤ 0.05	≤ 0.01	≤ 0.01	≤ 1

* Maximum Concentrations Limit (MCL) comes from Environmental announcement No.46 (Japan).

important factors that mainly influences the dissolution species of anions from fly ash. Rey et al. [23] found that when the pH increased more than 2.5, the dominant species of Se was transformed from H_2SeO_3 to SeO_3^{2-} which is more easily adsorbed on the surface of fly ash. Cr is highly depended on pH conditions where the acidic and extreme basic pH conditions showed higher leaching concentrations [24,25]. pH also controls the solubility of Ca minerals which immobilize anionic species. Hassett et al. [26] observed the weakening release of B from ettringite when the pH reached 11.5. Compared with pH, NOM with varying molecular weights and functional groups is a more complicated factor in its influence on the mobility of anions. Halim et al. [27] used acetic acid to simulate organic compounds in municipal landfill leachate and found that the mobility of Cr and As was inhibited through reduction reactions. Du et al. [28] found that the release of Cr was enhanced through its adsorption on solid humic acids in cement-solidified municipal solid waste incineration fly ash when the pH was lower than 7.0. Humic acid can increase the leaching of As by combining with metal ions to form nonadsorbable complexes [29]. The amine groups of humic acid played either inhibiting or enhancing roles in the retention of As, which depended on the acidic or alkaline environment [30]. Deonarine et al. [31] demonstrated that humic and fulvic acids could also enhance the mobility of As through competitive adsorption on mineral surfaces under oxic conditions. Therefore, the leachability of anionic species after the addition of Ca additives should be understood in the presence of NOM.

NOM includes fulvic acid, humic acid, and humins, which come from animal and plant residues in the pedosphere. The components of NOM include carbohydrates, amino acids, and proteins. Furthermore, amino acids are monomers of proteins with carboxyl and amine groups as well as small molecules. Therefore, in this work, five amino acids with varying side chain groups and acid dissociation constants (pK_a) were selected as simplified models of NOM to modify the dissolution tests. Different Ca additives including lime ($Ca(OH)_2$), gypsum ($CaSO_4$), and hydroxylated calcined dolomite ($Ca(OH)_2$, $Mg(OH)_2$), were used to improve Se, Cr, As, and B immobilization in fly ash blended cement systems. The fly ash blended cement was ground to explore the stability of anions at pH 4.7 and 12.0 to simulate acidic rain and realistic cement environments, respectively. After that, the effects of different amino acids on the dissolution behavior of Se, Cr, As, and B were discussed to provide a reference for the stability of undesirable anionic pollutants in fly ash blended cement.

2. Materials and methods

2.1. Materials

Fly ash was provided by an anonymous thermal power plant in Japan. Elemental compositions (mass%) were determined by X-ray fluorescence spectroscopy (XRF, Rigaku ZSX Primus II, Tokyo), as shown

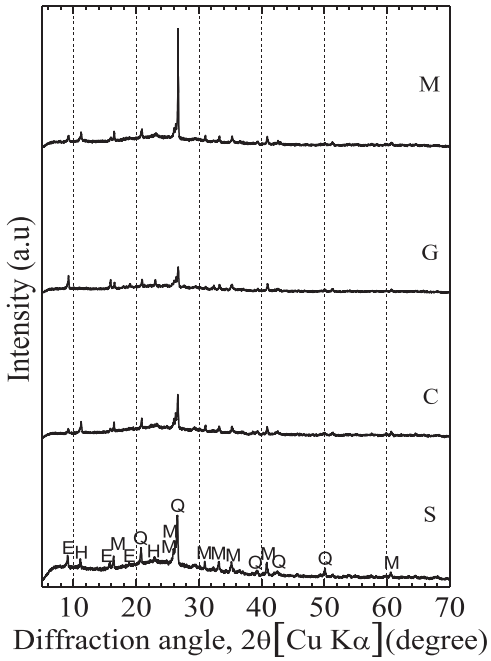

Fig. 1. XRD patterns of four cement blocks with S, C, G, M additives after curing for 28 d. E: ettringite ($Ca_6Al_2(OH)_{12}(SO_4)_3{\cdot}26\ H_2O$, PDF#01–075–7554); H: hydrocalumite ($3CaO{\cdot}Al_2O_3{\cdot}CaX_{2/m}{\cdot}nH_2O$, PDF# 01–078–2051); M: mullite ($Al_6O_{13}Si_2$, PDF#01–074–4143); Q:quartz (SiO_2, PDF#00–033–1161).

Table 4
Compositions of hydrocalumite and ettringite in initial fly ash-blended cement blocks.

Composition	S	C	G	M
Hydrocalumite/%	1.90	6.08	n.d.	4.12
Ettringite/%	2.16	1.09	6.09	1.81

n.d., not detected.

Table 3
Added amount of each material to prepare the fly ash-blended cement blocks (kg/m^3).

	S	C	G	M
Water	424	424	424	424
Cement	94	94	94	94
Fly ash	1219	1219	1219	1219
Ca additives	0	40 ($0.5398\ mol/m^3$, Ca^{2+})	40 ($0.2323\ mol/m^3$, Ca^{2+})	40 ($0.3478\ mol/m^3$, Ca^{2+})

S, C, G, and M represent cement without any Ca additives, with lime, gypsum, and hydroxylated calcined dolomite additives, respectively

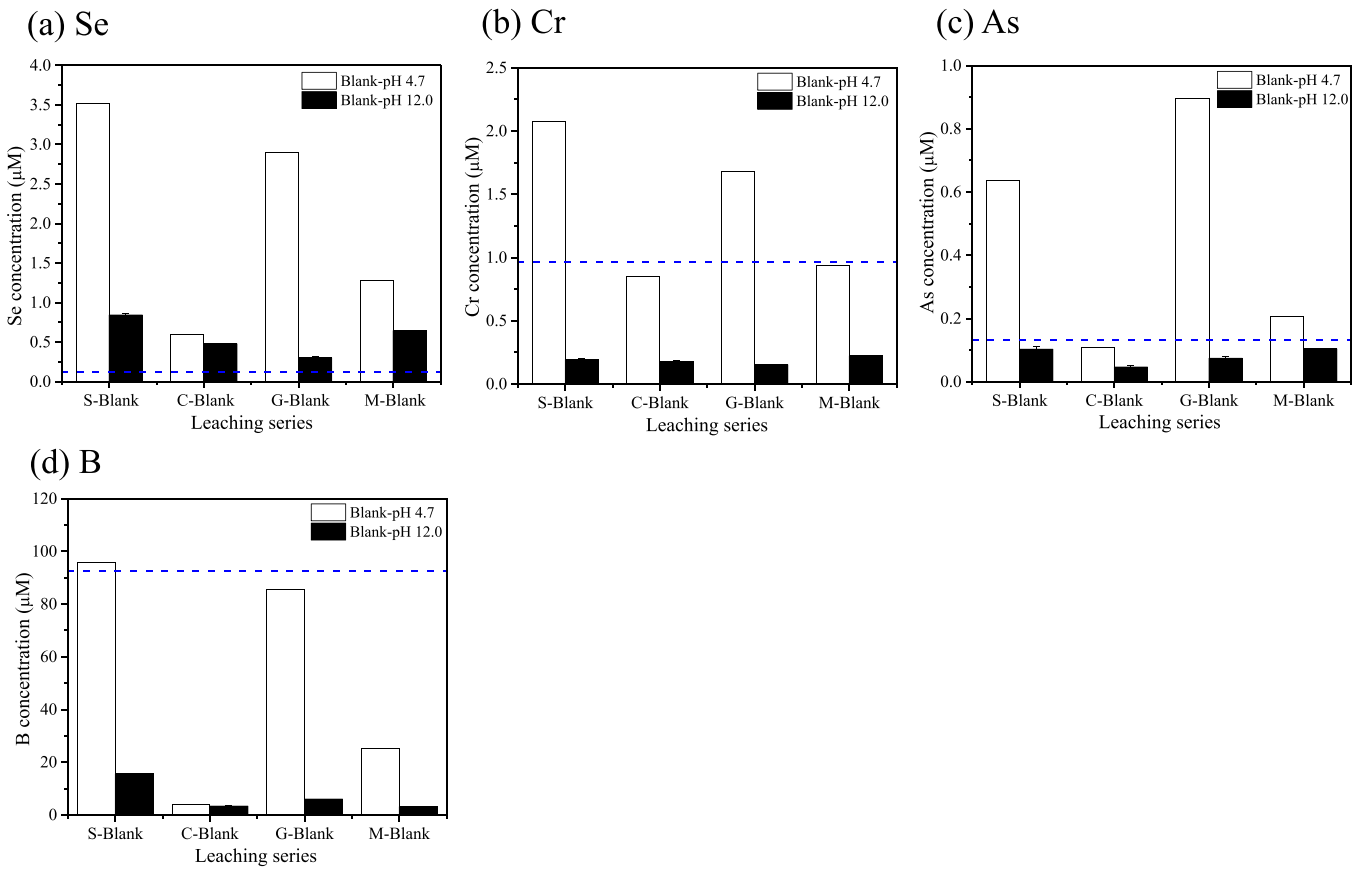

Fig. 2. Leaching results of (a) Se, (b) Cr, (c) As, and (d) B from grinding fly ash-blended cement powders in the absence of amino acids. Dotted lines indicate the maximum concentrations of limits (MCLs) according to Environmental Agency Notification No.46.

in Table 1. The dissolved Se, Cr, As, and B (Table 2) in the fly ash were extracted through acid digestion [17], which were measured and compared to criteria values in the Environmental Agency Notification No. 46 in Japan. However, the dissolved concentrations of Cr and Se were much higher than the regulatory limits, which indicates the existing risks associated with fly ash application. In this work, blast furnace cement containing 46.44% blast furnace slag was used. Ca additives, including lime, gypsum, and hydroxylated calcined dolomite, were added, separately. All the amino acids used in this work, including L-cysteine (H_2Cys, $C_3H_7NO_2S$, 99%), L-aspartic acid (H_2Asp, $C_4H_7NO_4$, 99%), glycine (HGly, $C_2H_5NO_2$, 99%), L-tryptophan (HTrp, $C_{11}H_{12}N_2O_2$, 99%), and L-phenylalanine (HPhe, $C_9H_{11}NO_2$, 99%) are of special grade. All the solutions were prepared using decarbonized Milli-Q water (integral water purification system, Millipore) that was boiled for 2 h with purging N_2 gas. NaOH (3 M) was used to adjust the pH of the solutions.

2.2. Preparation of fly ash blended cement

The Ca additives (40 kg/m^3) described above were added to the fly ash blended cement to improve the immobilization of hazardous elements, as shown in Table 3. In this work, the S, C, G, and M series denote cement without any Ca additives but with lime, gypsum, and hydroxylated calcined dolomite additives, respectively. The liquid/solid (L/S) mass ratio was fixed to 0.323. Following a previous procedure [17], the required amounts of cement, fly ash, and Ca additives were mixed. After curing for 28 days, the fly ash blended cement blocks were provided for compressive strength test according to JIS S1108 and then separately ground into powders under 280 mesh (53 μm) for further experiments.

2.3. Dissolution tests

A dissolution test was conducted with 1.0 g solid residue suspended in a 10 mL aqueous solution to determine the dissolved concentrations of Se, Cr, As, and B according to Environmental Agency Notification No.46 in Japan. The dissolution test was used as a regulatory tool to determine whether the fly ash blended cement wastes could be classified as hazardous or not. The extraction solution at pH 4.7 was 1 mM acetate buffer. Solutions of individual amino acids (5 mM) at pH 4.7 and pH 12.0 were also prepared for the dissolution test. The dissolution experiments were carried out at 200 rpm and 25 ℃ for 6 h in duplicate. After shaking for 6 h, the leachates were obtained, and solid residues were filtered through 0.45 μm pore size membrane filters and dried for further analysis. The leachates were used to measure pH and determine dissolved concentrations of hazardous elements.

2.4. Chemical analysis and solid characterization

The elemental compositions of fly ash were determined by XRF using a Rigaku ZSX Primus II (Akishima, Japan) in the wavelength dispersive mode: Rh-anode (3 or 4 kV, 60 kV). X-ray diffraction (XRD) patterns of solid samples were collected by Rigaku Ultima Ⅳ XRD (Akishima, Japan) using Cu Kα radiation (40 kV, 40 mA) at a scanning speed of 2° min^{-1} and with a scanning step of 0.02°. The Rietveld method was used to determine the mass contents of hydrocalumite and ettringite from the XRD patterns for each ground fly ash blended cement solid residue (90%, 900 mg) mixed with corundum (α-Al_2O_3) (10%, 100 mg) as an internal standard. The concentrations of the trace elements Se, Cr, As, and B were determined by inductively coupled plasma mass spectrometry (ICP-MS, Agilent 7500c). Under the current pH conditions, SeO_3^{2-}, CrO_4^{2-}, AsO_4^{3-}, and $B(OH)_4^-$ were the main species of Se, Cr, As, and B in

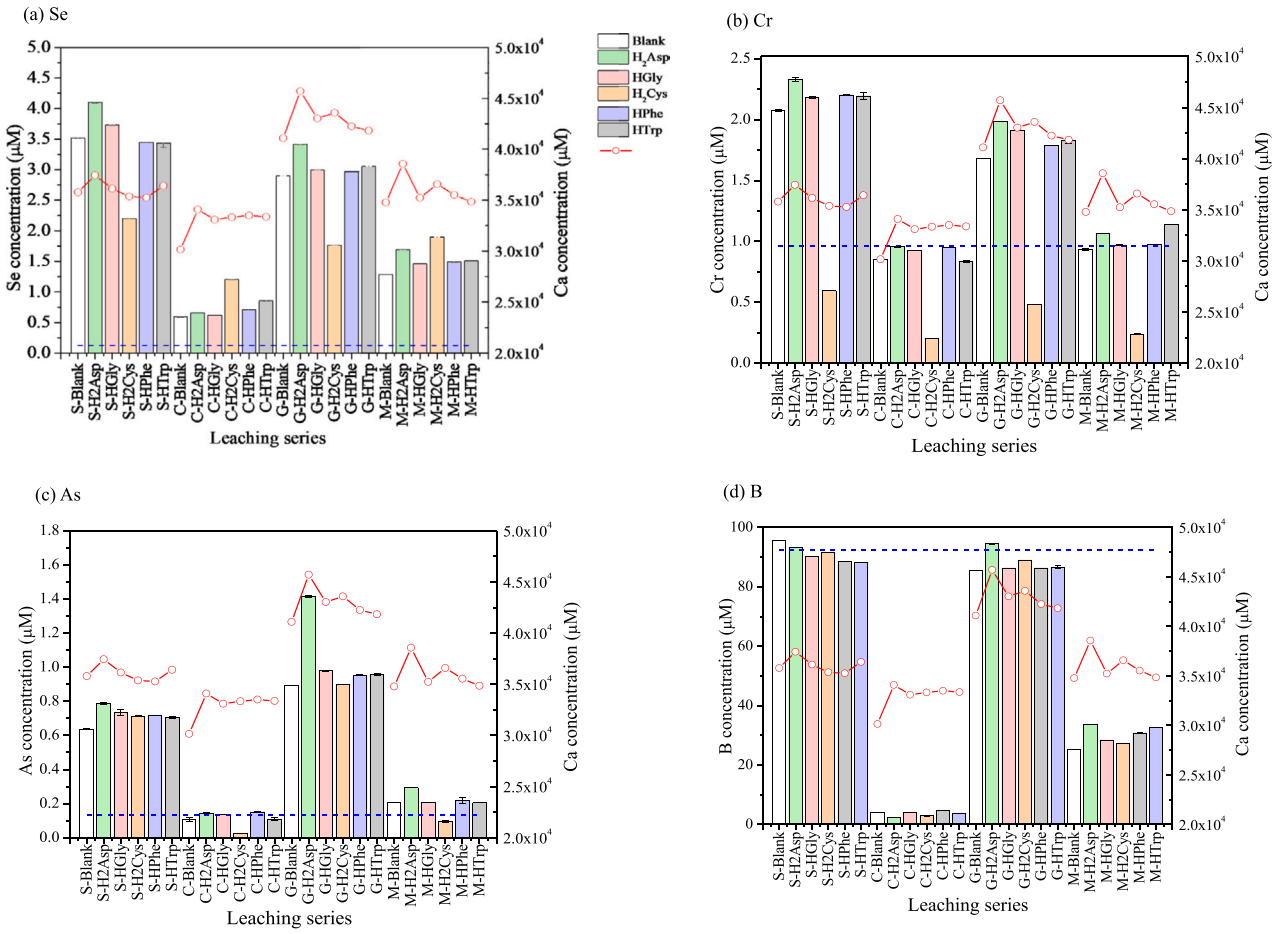

Fig. 3. Leaching concentrations of (a) Se, (b) Cr, (c) As, and (d) B from ground fly ash-blended cement powders in the presence of amino acids at the initial pH 4.7. Dotted lines indicate the maximum concentrations of limits.

leachates. Se(IV) was the dominant species of Se in fly ash, while Se(VI) was either absent or present in trace amounts.

3. Results and discussion

3.1. Characterization of ground fly ash blended cement powders

The role of Ca additives in the process of anionic species immobilization has been thoroughly explored in previous researches [17,19]. These studies showed that the excess amounts of Ca maintained the alkalization of the cement system and resulted in the good crystallization of hydrocalumite and ettringite. As shown in Fig. 1, the hydrocalumite ($K_{sp} = 3.72 \times 10^{-30}$, 25 ℃) and ettringite ($K_{sp} = 9.93 \times 10^{-45}$, 25 ℃) were formed as the hydration products in the presence of cement, fly ash, and Ca additives, which all play significant roles in immobilizing anionic species [32,33]. The amounts of SO_4^{2-} and Ca^{2+} decided these differences in hydrocalumite and ettringite formation. As shown in Table 3, 0.5398, 0.2323, and 0.3478 mol/m^3 of Ca^{2+} were present in the C, G, and M series, respectively. Thus, the addition of lime (C series) resulted in the highest Ca levels, followed by the addition of hydroxylated calcined dolomite (M series), and gypsum (G series). The amounts of hydrocalumite and ettringite affect the anionic removal capacities of cement systems. Therefore, combined with Fig. 1, the initial amounts of ettringite and hydrocalumite in each solid residue were estimated in Table 4. The content of ettringite in the G series increased to 6.09%, which was higher than that in the S (2.16%), M (1.81%), and C (1.09%) series. However, no hydrocalumite was detected. In the C and M series, approximately 6.08% and 4.12% of hydrocalumite were formed, respectively, and these values were significantly higher than those in the series without any Ca additives. Furthermore, the anionic removal capacity also is controlled by the structures of hydrocalumite and ettringite. Due to the flexibility of the interlayer distances of hydrocalumite, the charge and bonding characteristics determined anion preference in the order of $AsO_4^{3-} > SeO_3^{2-} > CrO_4^{2-} > B(OH)_4^-$ [32,34–36]. The changes in the coordination of tetrahedral $B(OH)_4^-$ to trigonal HBO_3^{2-} make it the lowest preference compared with the CrO_4^{2-}, SeO_3^{2-}, AsO_4^{3-} to hydrocalumite interlayer [32].

3.2. Effect of pH on the leachability of Se, Cr, As, and B

The levels of the undesirable elements Se, Cr, As, and B in the four series were determined using a dissolution test without amino acids at initial pH values of 4.7 and 12.0 (Fig. 2(a), (b), (c), and (d)). The blue dashed line represents the maximum concentrations of limits (MCLs). Without any additives, the eluted concentrations of Se, Cr, As, and B from ground fly ash blended cement exceeded the MCLs, but these concentrations decreased as the initial pH increased to 12.0. Even though hydrocalumite (Se/Cr/As/B) and ettringite (Se/Cr/As/B) have much lower K_{sp} values than Ca salts, their precipitation equilibrium is controlled by the contents of OH^-, that is, the solution pH. Therefore, at the initial pH of 4.7, hydrocalumite and ettringite in the ground fly ash blended cement dissolved and showed low intensities in the XRD patterns after being suspended for 6 h (Fig. S1). However, the dissolution of ettringite and hydrocalumite was reduced at pH 12.0 (Fig. S2), confirming their role in anionic species immobilization [37–39].

Compared to gypsum, the addition of lime and hydroxylated calcined dolomite more effectively inhibited the dissolution of Se, Cr, As, and B. At the initial pH of 4.7, the C series had the greatest inhibitory effect on

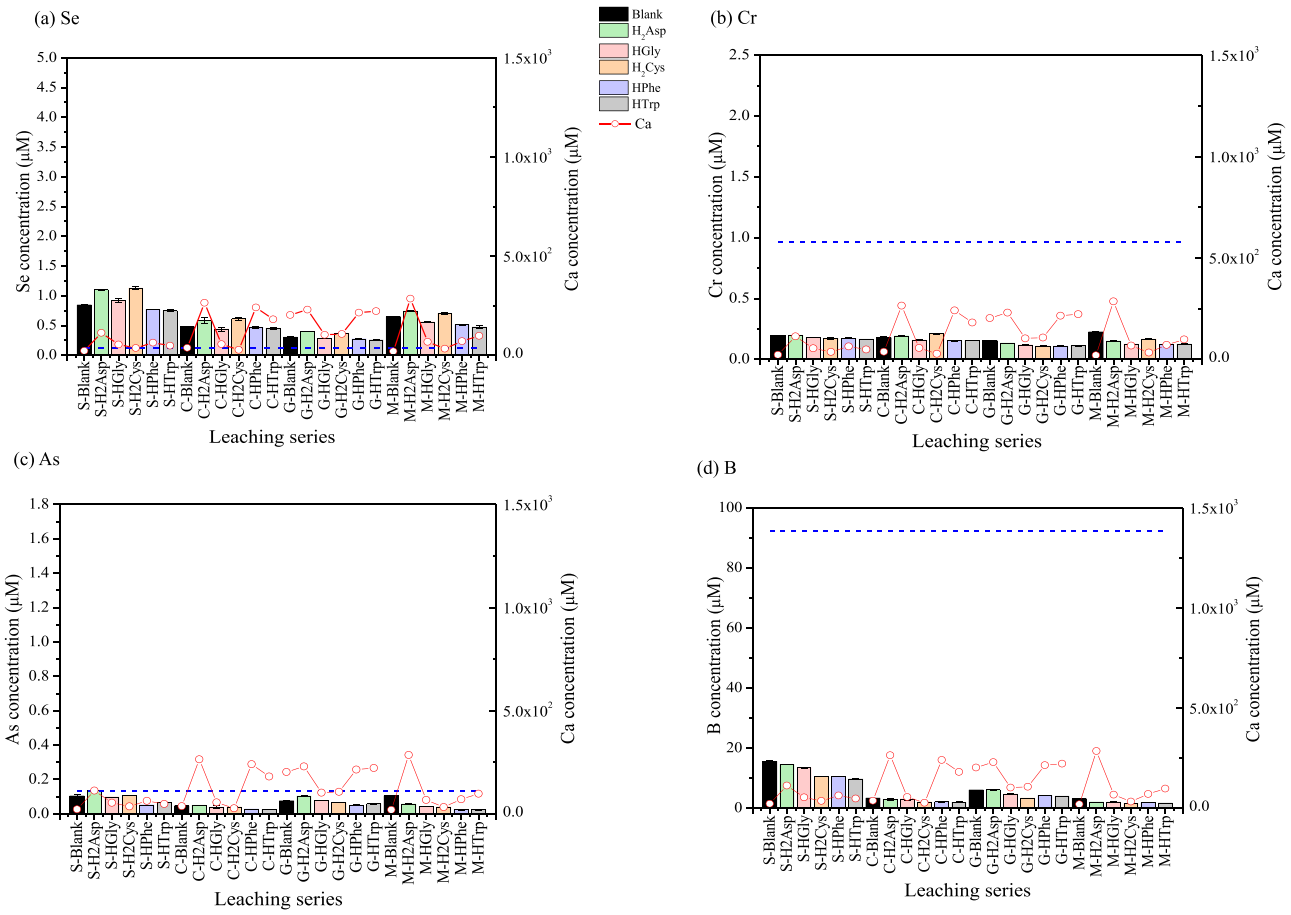

Fig. 4. Leaching concentrations of (a) Se, (b) Cr, (c) As, and (d) B from ground fly ash-blended cement powders in the presence of amino acids at the initial pH 12.0. Dotted lines indicate the maximum concentrations of limits.

the release of Se, Cr, As, and B. The presence of $CaSO_4$ increased the dissolution of As (Fig. 2**(c)**), which may be attributed to the competitive adsorption of SO_4^{2-} in ettringite [40]. This could also explain the exceeding standard behavior of Cr only in the G series. At the initial pH of 12.0, the dissolved concentrations of As, Cr, and B were sufficiently reduced to levels lower than the criteria values in all series. Even though Se had the lowest dissolution value in the G series, due to the competitive adsorption of AsO_4^{3-}, and SO_4^{2-} with SeO_3^{2-} in secondary minerals and the relatively higher K_{sp} (5.4×10^{-8}) of $CaSeO_3$, the dissolved concentration of Se was still higher than the criteria value. In the C series, the dissolution of B was well inhibited and seemed to be unaffected by changing of the pH in solutions. Considering the immobilization mechanisms of $B(OH)_4^-$, the contents of hydrocalumite and ettringite should be considered. The Ca^{2+} content has a significant impact on the release behavior of $B(OH)_4^-$. According to Fig. 5, the amount of hydrocalumite in the C series remained above 0.3% and provided sufficient adsorption sites for $B(OH)_4^-$. Therefore, this should explain the good immobilization of $B(OH)_4^-$. Additionally, in Fig. S3, the expanded figure of XRD results in the range of 8–25° in 2θ shows that hydrocalumite can still be detected in the presence of lime (C series). However, hydrocalumite disappears in the other series.

3.3. Role of amino acids on the leachability of Se, Cr, As, and B at the initial pH 4.7

The dissolved concentrations of Se, Cr, As, and B in ground fly ash blended cement treated in the presence of 5.0 mM amino acids at pH 4.7 are shown in Fig. 3. H_2Asp, HGly, HPhe, and HTrp exerted a promoting effect on Se, Cr, and As dissolution to different extents (Fig. 3(a), (b), (c)). H_2Cys also stimulated Se release but it played an inhibitory role in the S and G series. Due to the low stability of hydrocalumite and ettringite which is strongly dependent on solution pH, as shown in Eqs. (1) and (2), amino acids did not influence their formation.

$$6Ca^{2+} + 2Al(OH)_4^- + 3SO_4^{2-} + 4OH^- + 26\ H_2O = Ca_6Al_2(SO_4)_3(OH)_{12}{\cdot}26\ H_2O\ (K_{sp} = 9{\cdot}93\times10^{-45},\ 25\ ℃) \quad (1)$$

$$4Ca^{2+} + 2Al(OH)_4^- + SO_4^{2-} + 4OH^- + 6\ H_2O = Ca_4Al_2(OH)_{12}SO_4{\cdot}6\ H_2O\ (K_{sp} = 3{\cdot}72\times10^{-30},\ 25\ ℃) \quad (2)$$

Therefore, the ligand-promoted dissolution of Ca salts should be the mechanism that explains the above behaviors of amino acids. Amino acids are potential Ca-chelating ligands that function through their carboxyl and amine groups to prevent Ca salts precipitation, as shown in Eqs. (3)–(5). Several factors, such as charge density and ionic size, influence the stability constants of amino acid complexes. The carboxylic ($-COO^-$) and amine ($-NH_3^+$) groups in amino acids can interact with Ca^{2+} through the coordination of Ca-O and Ca-N. The Ca-O length was found to be much shorter than the Ca-N length, indicating that Ca^{2+} is prone to combine with the oxygen atoms in $-COO^-$ with a higher stable constant (K_{stab}) [41]. Since the stability constants are higher in Ca carboxyl complexes than Ca amine complexes, the hypothetical structure of carboxyl in amino acid complex with Ca^{2+} is only considered in Scheme 1(a). Among the amino acids, H_2Asp had the highest affinity for Ca^{2+}, which is consistent with its highest effect on promoting Se, Cr, and As release. Furthermore, a higher dissolved concentration of Ca^{2+} was detected in the H_2Asp amended dissolution test (Fig. 3), suggesting that H_2Asp is complexed with Ca^{2+}. The affinity also increases with an increase in solution pH. Thus, Ca^{2+} has a stronger affinity for

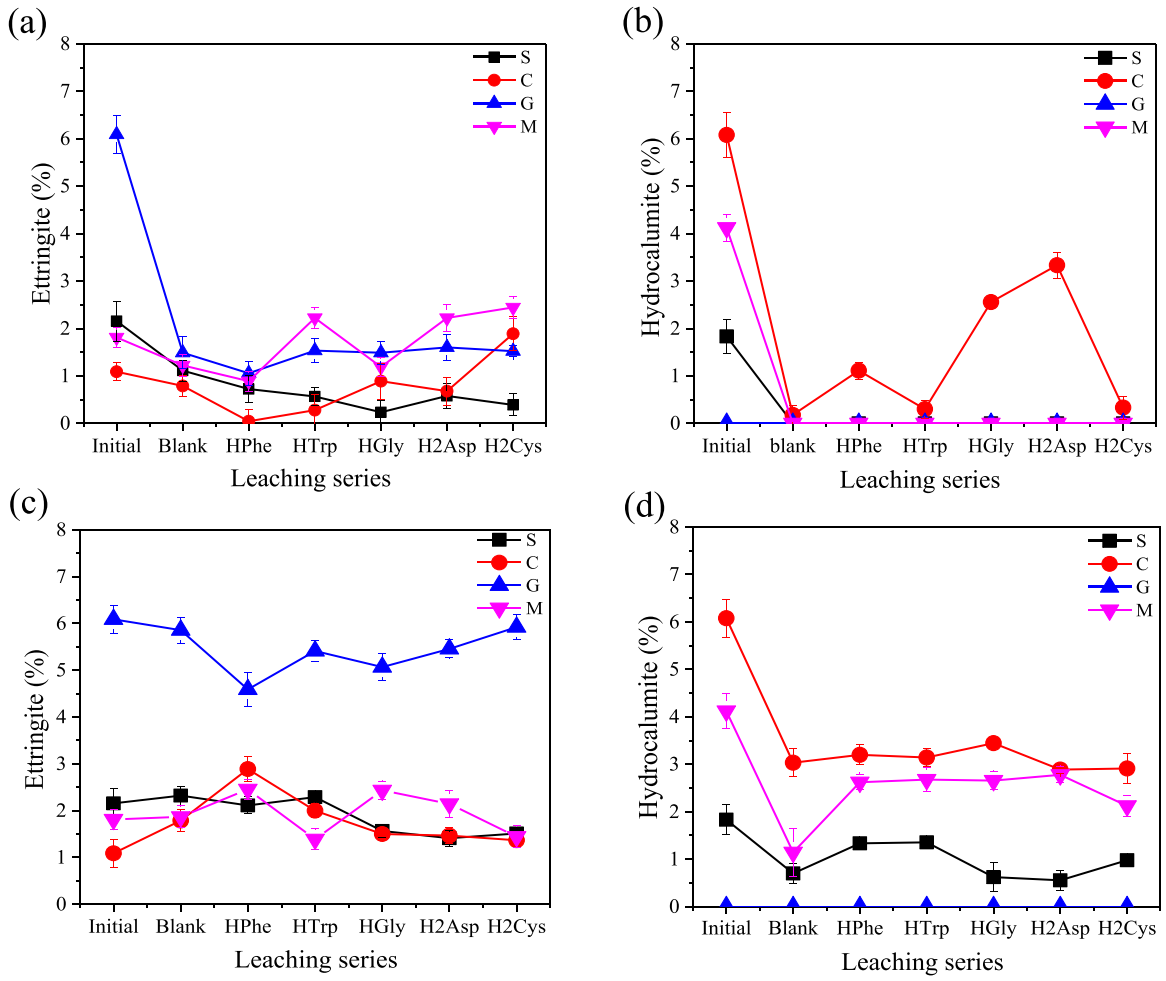

Fig. 5. Quantification of ettringite and hydrocalumite by Rietveld method in each cement block before and after amino acids dissolution tests under pH 4.7 and 12.0. (a) ettringite at pH 4.7, (b) hydrocalumite at 4.7, (c) ettringite at pH 12.0, (d) hydrocalumite at pH 12.0.

deprotonated amino acids in cement systems than in low pH systems where protonated amino acids are dominant. Even though Cys^{2-} possesses two negative charge numbers, it performed a weaker promoting effect compared with Asp^{2-}. The DFT simulations by Tang and Skibsted [42] confirmed that H_2Cys has a lower affinity for Ca^{2+} due to a longer Ca-O length in H_2Cys than in H_2Asp. Ca^{2+} is preferentially coordinated with two oxygen atoms of the -COO^- group in H_2Cys instead of -COO^- and -S^-, so the -SH group in H_2Cys does not affect Ca complex formation. Because the charges of HPhe and HTrp are lower than those of H_2Asp and H_2Cys, and also, they have larger molecular sizes, the affinity of them for Ca^{2+} is relatively low which can be confirmed by the Ca concentration in each coexisting amino acid leachate (Fig. 3).

$$Ca_3(AsO_4)_2 \rightleftharpoons 3Ca^{2+} + 2AsO_4^{3-} \ (K_{sp} = 6{\cdot}8\times10^{-19}) \quad (3)$$

$$CaCrO_4 \rightleftharpoons Ca^{2+} + CrO_4^{2-} \ (K_{sp} = 7{\cdot}1\times10^{-4}) \quad (4)$$

$$CaSeO_3 \rightleftharpoons Ca^{2+} + SeO_3^{2-} \ (K_{sp} = 5{\cdot}4\times10^{-8}) \quad (5)$$

In addition to complexation, H_2Cys seems to play another role. For -SH (pK_a = 8.18), it has one unpaired electron, making H_2Cys highly reactive in the free radical oxidation between two H_2Cys molecules, as shown in Eq. (6). H_2Cys can undergo an oxidation reaction under neutral or weakly alkaline conditions so that the two cysteine molecules gain electrons to form a cystine dimer. During this process, the oxidant that provides electrons can be reduced. Therefore, based on this, the decreasing dissolution concentrations of anions are related to the occurrence of redox reactions. Many experiments have been conducted to study the redox reaction potential. The obtained values are mostly in the range of − 0.23 to − 0.39 V [43–45], so they are cited in this paper as a reference of standard redox potential (E^0) values.

$$2\ C_3H_7NO_2S = C_6H_{12}N_2O_4S_2 + 2\ H^+ + 2e^- \ (E^0 = -0{\cdot}23\ V \sim -0{\cdot}39\ V) \quad (6)$$

Due to the dissolution of secondary Ca minerals such as $Ca(OH)_2$, hydrocalumite, and ettringite in the cement system, the pH of the solutions increased from 4.7 to approximately 9.0, as shown in Fig. S4. Under this condition, the carbonyl group of amino acids functions as a proton acceptor, while the amino group serves as a proton donor. Thus, the -NH_3^+ (pK_a =10.28) and -COO^- (pK_a =1.96) groups were produced in H_2Cys. As a result, H_2Cys can be oxidized to form a disulfide bond (S-S) between two H_2Cys molecules, as shown in Scheme 1(b). The E^0 of Se (IV)/Se(0) is − 0.366 V, which is a small difference from − 0.39 V (cysteine/cystine). Se is present in fly ash in trace amounts, so it is difficult to characterize fly ash blended cement in order to distinguish the existence of Se(0) species. Thus, according to Eq. (7), the reduction of Se(IV) to Se(0) may have occurred. However, the C and M series, in which excess amounts of Ca were introduced, immobilized more Se by forming ettringite, hydrocalumite, and $CaSeO_3$. Therefore, the low concentrations of dissolved Se have a weaker oxidation ability for participating in the redox reaction.

In the case of Cr in Fig. 3(b), H_2Cys inhibited its release and maintained its levels below the MLCs in all Ca additive series. CrO_4^{2-} is the dominant form in the alkaline region, and it has a weaker affinity than SeO_3^{2-} for hydrocalumite and ettringite. According to Eq. (8), the reduction of CrO_4^{2-} into Cr(III) occurred in the presence of H_2Cys

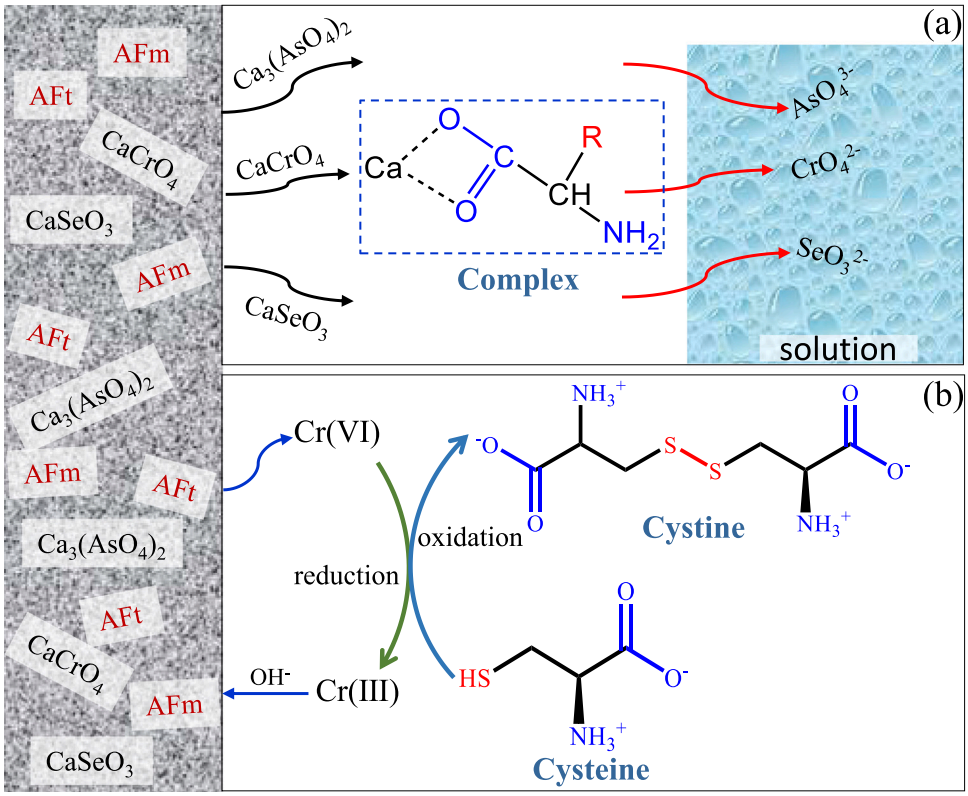

Scheme 1. Behaviors of amino acids in cement systems. (a) ligand promoted dissolution of Ca-amino acid, (b) redox reaction between cysteine and CrO_4^{2-}. E^0 values for Cr(VI)/Cr(III) and cysteine/cysteine are − 0.13 V and − 0.23 ~ − 0.39 V.

(Scheme 1(b)), leading to the precipitation of $Cr(OH)_3$ (K_{sp}=6.0 ×10^{-31}, 25 ℃). Dissolution of As(V) was effectively inhibited in the C and M series, but it was difficult for H_2Cys to reduce As(V) from AsO_4^{3-} to AsO_2^- (Eq. (9)). As shown in Fig. S1 and S2, in the presence of H_2Cys, lower amounts of ettringite were dissolved. However, in Fig. S4, the final pH of the H_2Cys series was lower than that of the other amino acids. Thus, in the C and M series, more Ca was dissolved from hydrocalumite due to its higher K_{sp} value (3.72 ×10^{-30}, 25 ℃) than ettringite (9.93 ×10^{-45}, 25 ℃) to facilitate $Ca_3(AsO_4)_2$ precipitation. Moreover, $Ca_4(OH)_2{\cdot}(AsO_4)_2{\cdot}4\,H_2O$ and $Ca_5(AsO_4)_3{\cdot}(OH)$ might be formed but only appear when the usable Ca amount is high [46,47]. None of the amino acids had significant effects on promoting the release of B (Fig. 3 (d)) compared with the blank series, confirming that ettringite and hydrocalumite are the main contributors that immobilize $B(OH)_4^-$ below the MCLs. However, the effects of amino acids on ettringite are still unclear.

$$SeO_3^{2-} + 3\,H_2O + 4e^- = Se^0 + 6OH^- \ (E^0 = -0{\cdot}366\ V) \quad (7)$$

$$CrO_4^{2-} + 4\,H_2O + 3e^- = Cr(OH)_3 + 5OH^- \ (E^0 = -0{\cdot}13\ V) \quad (8)$$

$$AsO_4^{3-} + 2\,H_2O + 2e = AsO_2^- + 4OH^- \ (E^0 = -0{\cdot}71\ V) \quad (9)$$

3.4. Role of amino acids on the leachability of Se, Cr, As, and B at the initial pH 12.0

When the initial pH of the amino acid solutions was 12.0, ettringite and hydrocalumite were stable in all the Ca additive cases (Fig. S2). In the G series, ettringite was still present in the highest amount, with more than 4.5% (Fig. S2(c)) showing the most efficient performance for immobilizing $B(OH)_4^-$ (Fig. 4(d)) among all Ca additive series. Because the pH was higher than the pK_a (-NH_3^+) in H_2Cys, oxidation of H_2Cys did not occur; correspondingly, the addition of H_2Cys did not decrease the dissolved concentrations of Se and Cr in fly ash (Fig. 4(a), (b)). It is obvious that the dissolved concentrations of Se, Cr, As, and B were sufficiently low to meet the MCLs, while the Se concentration remained above the criteria value. At pH 12.0, the -NH_3^+ (pK_a = 9.82) in H_2Asp was deprotonated to -NH_2, and the carboxyl groups (-COOH) were deprotonated to -COO^-. As a result, two negative charges were produced to Asp^{2-}. Similarly, H_2Cys behaved as Cys^{2-}. Asp^{2-} and Cys^{2-} enhanced the release of Se, suggesting that ligand-promoted dissolution by Ca-amino acid complexes destabilized SeO_3^{2-} in the Ca salts. However, because oxyanions were mainly coprecipitated in ettringite and hydrocalumite, the proportion of Ca salts in Se immobilization was greatly reduced. Moreover, in alkaline solutions, dissolution-reprecipitation and hydration consumed Ca, making it difficult to explain the contribution of this mechanism through the Ca^{2+} concentration, as shown in Fig. 4. Therefore, the ligand-promoted dissolution mechanism had no significant effect on enhancing the mobility of Cr and As species. In contrast, amino acids played an inhibitory role on the mobility of these species. Since hydrocalumite and ettringite were observed at abundant levels under alkaline conditions, the surface adsorption of amino acids on minerals caused by electrostatic adsorption should be considered. All the amino acids showed inhibitory effects on the release of B, even when present in trace amounts. Because $B(OH)_4^-$ is mainly incorporated in hydrocalumite and ettringite, amino acids affected their solubility through surface adsorption. The surface adsorption of amino acids can occur due to the positively charged surfaces of ettringite and hydrocalumite, and this behavior may weaken the dissolution of hydrocalumite and ettringite. In the presence of Gly^-, Phe^-, and Trp^-, the dissolution of Se was suppressed. Thus, the ion exchange of Asp^{2-} and Cys^{2-} with SeO_3^{2-} may have partially occurred to enhance the release of Se from the hydrocalumite interlayer. Even though SeO_3^{2-}, AsO_4^{3-}, and CrO_4^{2-} have strong affinities in hydrocalumite, high concentrations of Asp^{2-} and Cys^{2-} can be ionexchanged with SeO_3^{2-} to replace them. The lower negative charge numbers of Gly^-, Phe^- and Trp^- did not cause ion exchange with the above oxyanions.

4. Conclusions

The effects of different amino acids on the stability of undesirable anionic species in ground fly ash blended cement after adding different Ca additives were investigated using dissolution tests. Amino acids not only exerted promoting effects on the dissolution of Se, Cr, and As but also exerted inhibitory effects on these elements. At the initial pH 4.7, H_2Cys reduced the mobility of Cr(VI) and Se(IV) through a redox reaction. Furthermore, the deprotonated carboxyl groups (–COO^-) caused amino acids to be absorbed on the surface of ettringite and hydrocalumite by electrostatic attraction, reducing the leachability of undesirable anionic species. However, ligand-promoted dissolution of Ca^{2+} by amino acids enhanced the dissolution of undesirable elements (Se, Cr, and As) from ground fly ash blended cement even if Ca additives were added, particularly at an initial pH 4.7. When the initial pH of the amino acid solutions was 12.0, Asp^{2-} and Cys^{2-} with two negative charges may promote Se release by replacing with SeO_3^{2-} from the hydrocalumite interlayer, maintaining the stability of the hydrocalumite structure under alkaline conditions. However, compare to this model experiment, more complicated factors exist in the real geochemistry environment. Therefore, the behaviors of amino acids on the dissolution of Se, Cr, As, and B under more possible environmental conditions should be explored. Moreover, the corresponding measures to inhibit the dissolution of anionic species in fly ash should be clear in future studies.

CRediT authorship contribution statement

Mengmeng Wang: Conceptualization, Methodology, Formal analysis, Writing – original draft, Writing – review & editing, Validation. **Keiko Sasaki:** Conceptualization, Writing – review & editing, Funding acquisition, Supervision.

Declaration of Competing Interest

The authors declare that they have no known competing financial interests or personal relationships that could have appeared to influence the work reported in this paper.

Appendix A. Supporting information

Supplementary data associated with this article can be found in the online version at doi:10.1016/j.jece.2022.107926.

References

[1] R. Xu, T. Lyu, L. Wang, Y. Yuan, M. Zhang, M. Cooper, R.J.G. Mortimer, Q. Yang, G. Pan, Utilization of coal fly ash waste for effective recapture of phosphorus from waters, Chemosphere 287 (2022), 132431, https://doi.org/10.1016/j.chemosphere.2021.132431.

[2] Y.W. Chen, X. Yu, E. Appiah-Hagan, J. Pizarro, G.A. Arteca, L. Mercier, Q. Wei, N. Belzile, Utilization of coal fly ash and drinking water sludge to remove anionic As(V), Cr(VI), Mo(VI) and Se(IV) from mine waters, J. Environ. Chem. Eng. 6 (2018) 2470–2479, https://doi.org/10.1016/j.jece.2018.03.043.

[3] H. Zhou, R. Bhattarai, Y. Li, S. Li, Y. Fan, Utilization of coal fly and bottom ash pellet for phosphorus adsorption: Sustainable management and evaluation, Resour. Conserv. Recycl. 149 (2019) 372–380, https://doi.org/10.1016/j.resconrec.2019.06.017.

[4] Y. Luo, Y. Wu, S. Ma, S. Zheng, Y. Zhang, P.K. Chu, Utilization of coal fly ash in China: a mini-review on challenges and future directions, Environ. Sci. Pollut. Res. 28 (2021) 18727–18740, https://doi.org/10.1007/s11356-020-08864-4.

[5] J. Zhang, W. Dong, J. Li, L. Qiao, J. Zheng, J. Sheng, Utilization of coal fly ash in the glass–ceramic production, J. Hazard. Mater. 149 (2007) 523–526, https://doi.org/10.1016/j.jhazmat.2007.07.044.

[6] E. Shimizu, M.A. Promentilla, D.E. Yu, Utilization of coal fly ash and rice hull ash as geopolymer matrix-cum-metal dopant applied to visible-light-active nanotitania photocatalyst system for degradation of dye in wastewater, Catalysts 10 (2020), https://doi.org/10.3390/catal10020240.

[7] S. Boycheva, D. Zgureva, K. Lazarova, T. Babeva, C. Popov, H. Lazarova, M. Popova, Progress in the utilization of coal fly ash by conversion to zeolites with green energy applications, Materials 13 (2020), https://doi.org/10.3390/ma13092014.

[8] H. Wang, H. Li, X. Liang, H. Zhou, N. Xie, Z. Dai, Investigation on the mechanical properties and environmental impacts of pervious concrete containing fly ash based on the cement-aggregate ratio, Constr. Build. Mater. 202 (2019) 387–395, https://doi.org/10.1016/j.conbuildmat.2019.01.044.

[9] Q. Lu, X. Zhou, Y. Wu, T. Mi, J. Liu, B. Hu, Migration and transformation of lead species over CaO surface in municipal solid waste incineration fly Ash: a DFT study, Waste Manag. 120 (2021) 59–67, https://doi.org/10.1016/j.wasman.2020.11.011.

[10] X. Tian, F. Rao, C. Li, W. Ge, N.O. Lara, S. Song, L. Xia, Solidification of municipal solid waste incineration fly ash and immobilization of heavy metals using waste glass in alkaline activation system, Chemosphere 283 (2021), 131240, https://doi.org/10.1016/j.chemosphere.2021.131240.

[11] A.M. Balachandra, N. Abdol, A.G.N.D. Darsanasiri, K. Zhu, P. Soroushian, H. E. Mason, Landfilled coal ash for carbon dioxide capture and its potential as a geopolymer binder for hazardous waste remediation, J. Environ. Chem. Eng. 9 (2021), 105385, https://doi.org/10.1016/j.jece.2021.105385.

[12] X.D. Li, C.S. Poon, H. Sun, I.M.C. Lo, D.W. Kirk, Heavy metal speciation and leaching behaviors in cement based solidified/stabilized waste materials, J. Hazard. Mater. 82 (2001) 215–230, https://doi.org/10.1016/S0304-3894(00)00360-5.

[13] M. Izquierdo, X. Querol, Leaching behaviour of elements from coal combustion fly ash: an overview, Int. J. Coal Geol. 94 (2012) 54–66, https://doi.org/10.1016/j.coal.2011.10.006.

[14] G. Akar, M. Polat, G. Galecki, U. Ipekoglu, Leaching behavior of selected trace elements in coal fly ash samples from Yenikoy coal-fired power plants, Fuel Process. Technol. 104 (2012) 50–56, https://doi.org/10.1016/j.fuproc.2012.06.026.

[15] C.-C. Lu, M.H. Hsu, Y.-P. Lin, Evaluation of heavy metal leachability of incinerating recycled aggregate and solidification/stabilization products for construction reuse using TCLP, multi-final pH and EDTA-mediated TCLP leaching tests, J. Hazard. Mater. 368 (2019) 336–344, https://doi.org/10.1016/j.jhazmat.2019.01.066.

[16] M. Mahedi, B. Cetin, Leaching of elements from cement activated fly ash and slag amended soils, Chemosphere 235 (2019) 565–574, https://doi.org/10.1016/j.chemosphere.2019.06.178.

[17] K. Sasaki, S. Nakama, Q. Tian, B. Guo, M. Wang, R. Takagi, T. Takahashi, Elution characteristics of undesirable anionic species from fly ash blended cement in different aqueous solutions, J. Environ. Chem. Eng. 9 (2021), 105171, https://doi.org/10.1016/j.jece.2021.105171.

[18] W. Li, Y. Sun, M. Xin, R. Bian, H. Wang, Y. Wang, Z. Hu, H.N. Linh, D. Zhang, Municipal solid waste incineration fly ash exposed to carbonation and acid rain corrosion scenarios: Release behavior, environmental risk, and dissolution mechanism of toxic metals, Sci. Total Environ. 744 (2020), 140857, https://doi.org/10.1016/j.scitotenv.2020.140857.

[19] B. Guo, S. Nakama, Q. Tian, N.D. Pahlevi, Z. Hu, K. Sasaki, Suppression processes of anionic pollutants released from fly ash by various Ca additives, J. Hazard. Mater. 371 (2019) 474–483, https://doi.org/10.1016/j.jhazmat.2019.03.036.

[20] E.J. Reardon, S.Della Valle, Anion sequestering by the formation of anionic clays: lime treatment of fly ash slurries, Environ. Sci. Technol. 31 (1997) 1218–1223, https://doi.org/10.1021/es9607300.

[21] Q. Tian, B. Guo, S. Nakama, L. Zhang, Z. Hu, K. Sasaki, Reduction of undesirable element leaching from fly ash by adding hydroxylated calcined dolomite, Waste Manag 86 (2019) 23–35, https://doi.org/10.1016/j.wasman.2019.01.027.

[22] J. Kalembkiewicz, E. Sitarz-Palczak, Efficiency of leaching tests in the context of the influence of the fly ash on the environment, J. Ecol. Eng. 16 (2015) 67–80, https://doi.org/10.12911/22998993/589.

[23] J.R. Otero-Rey, M.J. Mato-Fernández, J. Moreda-Piñeiro, E. Alonso-Rodríguez, S. Muniategui-Lorenzo, P. López-Mahía, D. Prada-Rodríguez, Influence of several experimental parameters on As and Se leaching from coal fly ash samples, Anal. Chim. Acta 531 (2005) 299–305, https://doi.org/10.1016/j.aca.2004.10.029.

[24] M. Mahedi, B. Cetin, A.Y. Dayioglu, Effect of cement incorporation on the leaching characteristics of elements from fly ash and slag treated soils, J. Environ. Manag. 253 (2020), 109720, https://doi.org/10.1016/j.jenvman.2019.109720.

[25] W. Li, Y. Sun, Y. Huang, T. Shimaoka, H. Wang, Y. Wang, L. Ma, D. Zhang, Evaluation of chemical speciation and environmental risk levels of heavy metals during varied acid corrosion conditions for raw and solidified/stabilized MSWI fly ash, Waste Manag. 87 (2019) 407–416, https://doi.org/10.1016/j.wasman.2019.02.033.

[26] D.J. Hassett, D.F. Pflughoeft-Hassett, L.V. Heebink, Leaching of CCBs: observations from over 25 years of research, Fuel 84 (2005) 1378–1383, https://doi.org/10.1016/j.fuel.2004.10.016.

[27] C.E. Halim, J.A. Scott, H. Natawardaya, R. Amal, D. Beydoun, G. Low, Comparison between acetic acid and landfill leachates for the leaching of Pb(II), Cd(II), As(V), and Cr(VI) from cementitious wastes, Environ. Sci. Technol. 38 (2004) 3977–3983, https://doi.org/10.1021/es0350740.

[28] B. Du, J. Li, W. Fang, Y. Liu, S. Yu, Y. Li, J. Liu, Characterization of naturally aged cement-solidified MSWI fly ash, Waste Manag 80 (2018) 101–111, https://doi.org/10.1016/j.wasman.2018.08.053.

[29] S. Zhao, Z. Chen, J. Shen, J. Kang, J. Zhang, Y. Shen, Leaching mechanisms of constituents from fly ash under the influence of humic acid, J. Hazard. Mater. 321 (2017) 647–660, https://doi.org/10.1016/j.jhazmat.2016.09.054.

[30] P. Thanabalasingam, W.F. Pickering, Arsenic sorption by humic acids, Environ. Pollut. Ser. B Chem. Phys. 12 (1986) 233–246, https://doi.org/10.1016/0143-148X(86)90012-1.

[31] A. Deonarine, A. Kolker, M.W. Doughten, J.T. Holland, J.D. Bailoo, Mobilization of arsenic from coal fly ash in the presence of dissolved organic matter, Appl. Geochem. 128 (2021), 104950, https://doi.org/10.1016/j.apgeochem.2021.104950.

[32] M. Zhang, E.J. Reardon, Removal of B, Cr, Mo, and Se from wastewater by incorporation into hydrocalumite and ettringite, Environ. Sci. Technol. 37 (2003) 2947–2952, https://doi.org/10.1021/es020969i.
[33] C.J. Warren, E.J. Reardon, The solubility of ettringite at 25°C, Cem. Concr. Res. 24 (1994) 1515–1524, https://doi.org/10.1016/0008-8846(94)90166-X.
[34] F.L. Theiss, G.A. Ayoko, R.L. Frost, Removal of boron species by layered double hydroxides: a review, J. Colloid Interface Sci. 402 (2013) 114–121, https://doi.org/10.1016/j.jcis.2013.03.051.
[35] S.C.B. Myneni, S.J. Traina, G.A. Waychunas, T.J. Logan, Vibrational spectroscopy of functional group chemistry and arsenate coordination in ettringite, Geochim. Cosmochim. Acta 62 (1998) 3499–3514, https://doi.org/10.1016/S0016-7037(98)00221-X.
[36] F.P. Glasser, The role of sulfate mineralogy and cure temperature in delayed ettringite formation, Cem. Concr. Compos. 18 (1996) 187–193, https://doi.org/10.1016/0958-9465(96)00015-7.
[37] K. Piekkari, K. Ohenoja, V. Isteri, P. Tanskanen, M. Illikainen, Immobilization of heavy metals, selenate, and sulfate from a hazardous industrial side stream by using calcium sulfoaluminate-belite cement, J. Clean. Prod. 258 (2020), 120560, https://doi.org/10.1016/j.jclepro.2020.120560.
[38] Y. Tsunashima, A. Iizuka, J. Akimoto, T. Hongo, A. Yamasaki, Preparation of sorbents containing ettringite phase from concrete sludge and their performance in removing borate and fluoride ions from waste water, Chem. Eng. J. 200–202 (2012) 338–343, https://doi.org/10.1016/j.cej.2012.06.064.
[39] T. Hongo, Y. Tsunashima, A. Iizuka, A. Yamasaki, Synthesis of anion-exchange materials from concrete sludge and evaluation of their ability to remove harmful anions (borate, fluoride, and chromate), Int. J. Chem. Eng. Appl. 5 (2014) 298–302, https://doi.org/10.7763/ijcea.2014.v5.397.
[40] M. Chrysochoou, D. Dermatas, Evaluation of ettringite and hydrocalumite formation for heavy metal immobilization: literature review and experimental study, J. Hazard. Mater. 136 (2006) 20–33, https://doi.org/10.1016/j.jhazmat.2005.11.008.
[41] P.H. Qin, W. Zhang, W.C. Lu, Theoretical study of hydrated Ca^{2+}-amino acids (glycine, threonine and phenylalanine) clusters, Comput. Theor. Chem. 1021 (2013) 164–170, https://doi.org/10.1016/j.comptc.2013.07.005.
[42] N. Tang, L.H. Skibsted, Calcium binding to amino acids and small glycine peptides in aqueous solution: toward peptide design for better calcium bioavailability, J. Agric. Food Chem. 64 (2016) 4376–4389, https://doi.org/10.1021/acs.jafc.6b01534.
[43] P.C. Jocelyn, The standard redox potential of cysteine-cystine from the thiol-disulphide exchange reaction with glutathione and lipoic acid, Eur. J. Biochem. 2 (1967) 327–331, https://doi.org/10.1111/j.1432-1033.1967.tb00142.x.
[44] G. Gorin, G. Doughty, Equilibrium constants for the reaction of glutathione with cystine and their relative oxidation-reduction potentials, Arch. Biochem. Biophys. 126 (1968) 547–551, https://doi.org/10.1016/0003-9861(68)90440-2.
[45] S. Bannai, Transport of cystine and cysteine in mammalian cells, Biochim. Biophys. Acta Rev. Biomembr. 779 (1984) 289–306, https://doi.org/10.1016/0304-4157(84)90014-5.
[46] D.H. Moon, D. Dermatas, N. Menounou, Arsenic immobilization by calcium–arsenic precipitates in lime treated soils, Sci. Total Environ. 330 (2004) 171–185, https://doi.org/10.1016/j.scitotenv.2004.03.016.
[47] Y. Zhu, X. Zhang, Q. Xie, Y. Chen, D. Wang, Y. Liang, J. Lu, Solubility and stability of barium arsenate and barium hydrogen arsenate at 25°C, J. Hazard. Mater. 120 (2005) 37–44, https://doi.org/10.1016/j.jhazmat.2004.12.025.